

# Absolute Angle and Glass Thickness Measurement Based on Dispersive Interferometry

Bo Peng<sup>1</sup>, Xinghua Qu, Fumin Zhang<sup>1</sup>, Guoqing Tang, Tianyu Zhang, and Xianyu Zhao

**Abstract**—Method to accurately measure both refractive index and the thickness of glass is investigated. The method combines equal inclination interference with dispersive interferometry. The interference signal, which is detected by the spectrometer, contains different frequencies and can be demodulated with high accuracy. The experiments indicate that the standard deviation of the thickness is better than the 35 nm, while the standard deviation of the measured refractive indices is below  $5.76 \times 10^{-6}$ . Furthermore, absolute angles, between  $0^\circ$  and  $51^\circ$ , can be measured with a repeatability within  $5''$ .

**Index Terms**—Ultrafast optics, measurement, dispersive interferometry, EIIT.

## I. INTRODUCTION

OPTICAL frequency combs are used in many areas such as precision spectroscopy [1], dimensional measurements [2], and 3D measurements [3]. In the year 2000, Minoshima and Matsumoto proposed the first absolute distance measurement system based on frequency combs [4], and performed a very accurate measurement of a long distance. Subsequently, several novel geometric measurement methods were published, including time of flight [5], dispersive interferometry [6], [7], multi-heterodyne interferometry [8], [9], and pulse cross-correlation [10], [11]. Dispersive interferometry was proposed by Ki-Nam Joo and Seung-Woo Kim in 2006, and, although it is very stable, it is difficult to perform arbitrary, long-distance measurements. In 2007, the refractive index of glass was measured using a spectrally resolving interferometer [12]. This represented a new application for femtosecond pulses, and an air refractometer, which uses this technique, was built and investigated [13].

Because refractive index and thickness are two key properties of optical materials, the precise measurement of these two factors is important. Accurate measurements of these two properties can already be performed via, for example, goniometry, ellipsometry, reflectometry and confocal microscopy. In addition, low-coherence interferometry [14], [15] was used to measure the optical thickness to obtain the group refractive index and the geometrical thickness of the sample. Unfortunately, compared to dispersive interferometry, these methods are complex and difficult to execute.

Manuscript received June 13, 2019; accepted June 23, 2019. Date of publication June 28, 2019; date of current version July 17, 2019. (Corresponding author: Fumin Zhang.)

B. Peng, X. Qu, F. Zhang, G. Tang, and X. Zhao are with Tianjin University, Tianjin 300072, China (e-mail: zhangfumin@tju.edu.cn).

T. Zhang is with the Shenyang Institute of Automation, Shenyang 110016, China.

Color versions of one or more of the figures in this letter are available online at <http://ieeexplore.ieee.org>.

Digital Object Identifier 10.1109/LPT.2019.2925690

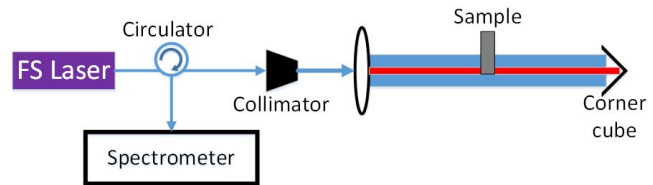


Fig. 1. Schematic of the setup for the glass-thickness measurement.

In this letter, a measurement system, which uses dispersive interferometry, is designed and built to measure both geometric thickness and refractive index simultaneously. The method can also improve the signal-to-noise ratio (SNR) for equal inclination interference by using a corner cube as reflector. Furthermore, a method for absolute angle measurements is proposed. By demodulating the interference signal, which is obtained by the spectrometer, both thickness and refractive index of the glass can be measured with high accuracy. The angle of incidence of the femtosecond pulse can also be derived from the optical path difference (OPD).

## II. DESIGN AND MEASUREMENT

The setup for this measurement is shown in Figure 1. Different from a conventional Michelson interferometer, the reference- and measurement-arms consist of parallel beams (shown in red and blue), even though the sample surface is not aligned perpendicular to the pulse laser. This measurement setup requires fewer mechanical parts, which makes it more compact and stable. The femtosecond pulse-laser source used in our experiment is a One-Five Origami –15 with a repetition frequency of 250MHz, and the femtosecond pulse spans a spectral width of 14.8 THz, with a central wavelength of 1560 nm. The spectrometer is a YOKOGAWA AQ6370D with a highest resolution of 0.02 nm, and the maximum non-ambiguity range (NAR) of this ranging system is about 300 mm. A collimator and a lens are used to expand the beam emitted from the circulator, while the beams reflected by the sample and corner cube are detected by the spectrometer after passing through a circulator. The corner cube and the sample represent a resonant cavity, which can increase the number of reflections within the glass sample. And the cavity improves the modulation depth and the signal-to-noise ratio for dispersive interferometry. All samples used in this experiment are flat windows without coating.

The spectral power density  $I(\nu)$  obtained by the spectrometer can be described as:

$$I(\nu) = a(\nu)[1 + \cos(2\pi\nu\tau)], \quad (1)$$

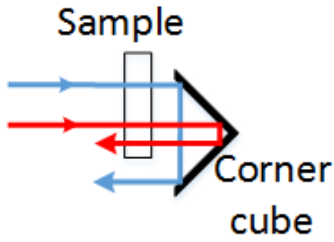


Fig. 2. Optical path of the emerging beam when the sample doesn't cover the corner cube completely.

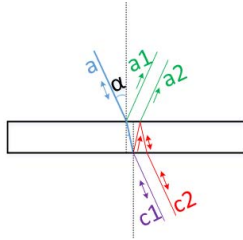


Fig. 3. Optical path of the laser beam passing through the glass sample.

where  $\nu$  and  $\tau$  denote the optical frequency and time delay, respectively. Furthermore,  $a(\nu)$  is the normalized intensity of the interference signal and  $\tau$  can be formulated as:

$$\tau = 2L/c, \quad (2)$$

with  $c$  and  $L$  being the speed of light in vacuum and the OPD, respectively. The spectral density  $I(\nu)$  is modulated by a signal with the frequency  $\tau$ .

The femtosecond laser-pulse, which is emitted from the source, is broadened by the beam-expansion structure. The emerging light-beam can be split into several beams with different optical paths, using the sample and the reflector. The optical distances of these beams are directly affected by the sample and the reflector. We adjust the position of the sample to ensure that the center of the laser transmits the sample as shown in Figure 2. As a result, one light beam (shown in blue) passes through the sample only once, while another light beam (shown in red) passes the sample twice. The OPD between these two beams can be described using

$$L_1 = D(n_s - n_a), \quad (3)$$

where  $D$  is the geometrical thickness of the sample,  $n_s$  and  $n_a$  denote the refractive indices of sample and air, respectively. However, if the corner cube is replaced by the mirror, the reference and measurement beams return on the original path, and the OPD  $L_1$  needs to be described as  $L_1 = 2D(n_s - n_a)$ .

As shown in Figure 3, some of the light that transmits the sample (shown in red) is reflected within the sample, while part the beam (shown in purple) is not reflected. In this experiment, a corner cube is used behind the sample (Figure 1), such that the beams  $c_1$ ,  $c_2$ ,  $a_1$ ,  $a_2$  can return to the collimator together, which can improve the modulation depth of the interference spectrum. When the glass thickness is measured, the angle of incidence,  $\alpha$ , is  $0^\circ$ . The OPD of these two beams ( $c_1$  and  $c_2$ ), can be expressed as

$$L_2 = mDn_s, \quad (4)$$

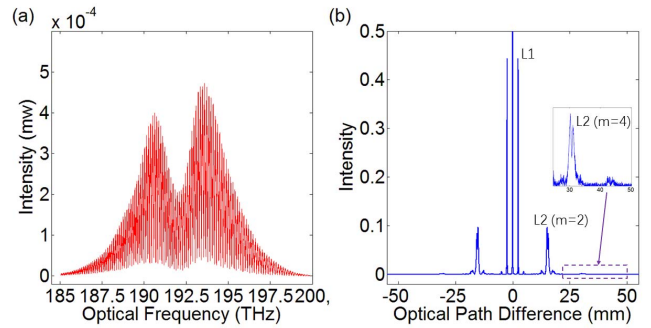


Fig. 4. (a) Interference signal of the glass-thickness measurement. (b) Fourier-transformed signals of the spectrum ( $m$  denotes the number of times the beams are reflected within the sample).

where  $m$  denotes the number of times the beams are reflected within the sample, which is an even number. Part of the laser (shown in green) is reflected at the front- and rear-surfaces, and the corresponding OPD for  $a_1$  and  $a_2$  is  $L_2$  too.

Clearly, when the emerging beam is perpendicular to the sample, with respect to equal inclination interference, the OPD between the measurement and reference arms in this experiment depends mainly on three factors: refractive index of air, geometrical thickness, and refractive index of the sample. The OPDs,  $L_1$  and  $L_2$ , in this experiment are independent of the position of the corner cube, which can improve the stability of the measurement. In this ranging system, the spectrum of the femtosecond pulse is modulated by different frequencies which are related to the OPDs,  $L_1$  and  $L_2$ , and the spectral power density  $I(\nu)$  can be rewritten as:

$$I(\nu) = \sum a_p(\nu) [1 + \cos(2\pi\nu\tau_p)], \quad (5)$$

where the index  $p$  is used to distinguish the different modulation frequencies. More precisely, the dispersive interference signal has many modulation frequencies, which can be neglected compared to  $L_1$  and  $L_2$ . The experimental results indicate that the decomposition of the dispersive interference signals is not complex. The intensity of each modulation frequency can be adjusted by adjusting the position of the sample in Figure 2. To ensure the sample surface is perpendicular to the emerging beam, the alignment of the sample and the collimator should be adjusted when the path to the corner cube is blocked.

Figure 4(a) shows the modulated spectrum obtained by the spectrometer. The modulation depth depends on the reflectivity of the glass and the resolution of the spectrometer. The reflectivity of the glass surface affects the intensity ratio between reference- and measurement-beam. The resolution of the spectrometer affects the sampling line width, and the modes can be sampled. In addition, it determines the coherence of the beams and the NAR of the measurement system. The modulation frequencies do not fold in this experiment because the optical thickness of the sample is shorter than the maximum NAR. The Fourier-transformed signal of the spectrum is shown in Figure 4(b).

There are different frequencies, which correspond to different factors  $m$ , which can be observed. In other words, different kinds of OPD ( $L_2$ ) can be detected. Both OPD  $L_1$  and  $L_2$

TABLE I  
RESULTS OF THE THICKNESS AND REFRACTIVE INDEX MEASUREMENT

Sample	WG42012	WG10530	WG41050
Reference thickness(mm)	12.0 ± 0.3	5.0 ± 0.3	5.0 ± 0.3
Thickness (mm)	11.767460	5.091544	5.179108
Standard deviation (nm)	32	22	28
Refractive index	1.479338	1.523179	1.465872
Standard deviation	3.61 × 10 <sup>-6</sup>	5.54 × 10 <sup>-6</sup>	5.76 × 10 <sup>-6</sup>

relate to the frequency components of the interferometer signal [6], and the time delay can be calculated using Eq. (2) and Eq. (5). By observing Eq. (3) and Eq. (4), we can know that OPD is single-valued, while OPD has several values. The value of  $L_1$  is smaller than  $L_2$  at all times. And the modulation frequencies can be distinguished with each other. The geometrical thickness of the glass in the measurement setup shown in Figure 2 can be derived with the simultaneous equations of Eq. (3) and Eq. (4):

$$D = (L_2 - mL_1) / mm_a, \quad (6)$$

Furthermore, the refractive index of the glass  $n_s$  can be determined by

$$n_s = L_2 / mD, \quad (7)$$

Table 1 shows the measurement results for the geometric thickness and the refractive index of the glasses. We get the reference value from the instructions of the samples. The environment conditions were 23.63 °C, 1018.6 hPa, and 34.59% humidity. The refractive index of air  $n_a$  is 1.0002894, using the modified Edlén formula [16]. Three different glasses WG42012 (UVFS), WG41050 (UVFS), and WG10530 (N-BK7), were measured 10 times, in fast succession, in our experiment. The standard deviations of the measurement results for the geometric thicknesses are: 32 nm, 22 nm, and 28 nm respectively, with standard deviations for the refractive indices of  $3.61 \times 10^{-6}$ ,  $5.54 \times 10^{-6}$ , and  $5.76 \times 10^{-6}$ , respectively.

Furthermore, a method for absolute angle measurement, which is based on dispersive interferometry, is demonstrated. As shown in Figure 5, the light received by the collimator is sufficiently intense (due to the reflector), even though the sample surface is not perpendicular to the emerging light beam. Here,  $\alpha$  is the angle of incidence, and  $\beta$  is the refraction angle. The relationship between  $\alpha$  and  $\beta$  can be determined using Snell's law. A measurement of  $L_1$  is not required when measuring the incident angle, and it is preferable to let all the emerging light pass through the sample by shifting the sample – see Figure 5. Like equal inclination interference, the laser pulse is reflected within the sample, the OPD of the light shown in Figure 5, in red and blue, can be expressed as:

$$L_3 = (2\Delta L - d)m/2, \quad (8)$$

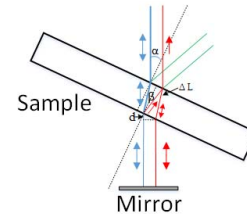


Fig. 5. Optical path within the glass, when the emerging beam is not perpendicular to the glass surface.

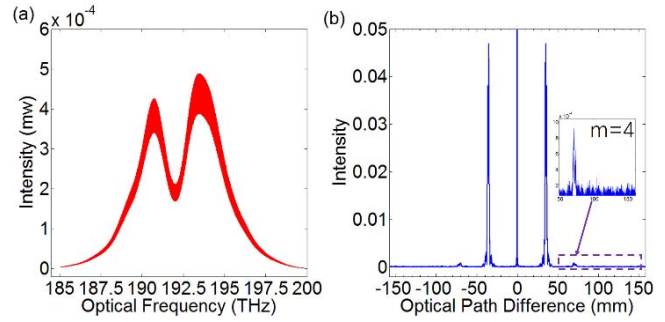


Fig. 6. (a) The interference signal of the angle measurement (the angle of incidence is about 12°). (b) Fourier-transformed signals of the spectrum.

where  $\Delta L$ , is given by  $\Delta L = Dn_s / \cos \beta$ ,  $d$  is given by  $d = 2 Dn_a \tan \beta \sin \alpha$ , and the even integer number denotes the number of reflections within the sample. When the factor  $m$  is equal to 2, the OPD  $L_3$  can be derived as follows:

$$L_3 = 2Dn_s \sqrt{1 - (n_a \sin \alpha / n_s)^2}, \quad (9)$$

where both thickness and refractive index of the glass can be measured accurately using the method shown above. The angle of incidence  $\alpha$  can be determined using  $L_3$ . The sine  $\alpha$  of can formulated as:

$$|\sin \alpha| = \frac{n_s}{n_a} \sqrt{1 - \left( \frac{L_3}{2Dn_s} \right)^2}, \quad (10)$$

Because the angle of incidence cannot exceed 90 degrees,  $|\sin \alpha| = \sin \alpha$ . The angle  $\alpha$  can be determined using the above equation.

The OPD of the beams, which is reflected by the front and rear surfaces (shown in green), is also equal to  $L_3$ . However, the reflected light requires another collimator to be received. Because it is hard to perform the measurement when the incident angle  $\alpha$  varies continuously, the reflector is required for continuous angle measurements. The sample is fixed on a rotatable platform, which can be used to change the angle of incidence of the emerging beam. The axis of the platform remains perpendicular to the emerging light beam during the entire experiment. The interference signal detected by the spectrometer is shown in Figure 6. The modulation depth becomes shallower because the interference signal does not contain the modulation frequency related to  $L_1$ . The intensity of the light (in red), shown in Figure 5, is weaker a lot than the light shown in blue. Figure 6(b) shows the Fourier-transformation of the interference signal.

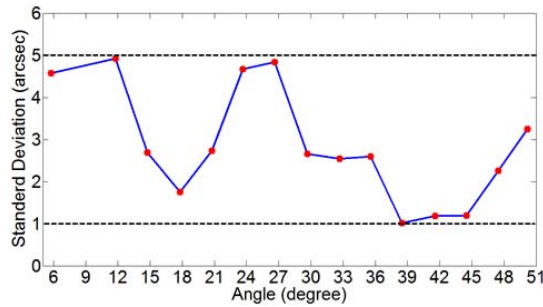


Fig. 7. Standard deviation of the absolute angle measurement.

According to Figure 6(b), the value of  $L_3$  can be determined using Eq. (2) and Eq. (4). The sample, WG42012 (UVFS), was used to determine the feasibility of the angle measurement. Figure 7 shows the standard deviations of the angle measurements. The glass was rotated from  $0^\circ$  to  $51^\circ$  clockwise, at intervals of about  $3^\circ$ , 5 times in rapid succession, to measure at each position. The repeatability of the measurement results varies from 1" to 5". The system setup is symmetric, which means that this method can also be used to measure the angle of incidence, when the sample rotates anticlockwise. As a result, the range for absolute angle measurements is  $-51^\circ$  to  $51^\circ$ . The range for the measurable angle of incidence can increase when the diameter of the sample increases or the diameter of the emerging light decreases.

### III. CONCLUSIONS

By combining equal inclination interference with dispersive interferometry, a stable compact measurement-setup was designed and built to measure both refractive index and geometric thickness of glass samples. The measurement procedure was simplified substantially. Three different glass samples were measured with high repeatability. Furthermore, a method for absolute angle measurements was introduced, and angles of incidence, ranging from  $0^\circ$  to  $51^\circ$ , were measured accurately.

### REFERENCES

- [1] I. Coddington, N. Newbury, and W. Swann, "Dual-comb spectroscopy," *Optica*, vol. 3, no. 4, pp. 414–426, 2016.
- [2] J. Jonghan, "Dimensional metrology using the optical comb of a mode-locked laser," *Meas. Sci. Technol.*, vol. 27, no. 2, Dec. 2016, Art. no. 022001.
- [3] T. Kato, M. Uchida, and K. Minoshima, "No-scanning 3D measurement method using ultrafast dimensional conversion with a chirped optical frequency comb," *Sci. Rep.*, vol. 7, Jun. 2017, Art. no. 3670.
- [4] K. Minoshima and H. Matsumoto, "High-accuracy measurement of 240-m distance in an optical tunnel by use of a compact femtosecond laser," *Appl. Opt.*, vol. 39, no. 30, pp. 5512–5517, 2000.
- [5] J. Ye, "Absolute measurement of a long, arbitrary distance to less than an optical fringe," *Opt. Lett.*, vol. 29, no. 10, pp. 1153–1155, 2004.
- [6] K.-N. Joo and S.-W. Kim, "Absolute distance measurement by dispersive interferometry using a femtosecond pulse laser," *Opt. Express*, vol. 14, no. 13, pp. 5954–5960, 2006.
- [7] M. Cui, M. G. Zeitouny, N. Bhattacharya, S. A. van den Berg, and H. P. Urbach, "Long distance measurement with femtosecond pulses using a dispersive interferometer," *Opt. Express*, vol. 19, no. 7, pp. 6549–6562, 2011.
- [8] R. Yang, F. Pollinger, K. Meiners-Hagen, J. Tan, and H. Bosse, "Heterodyne multi-wavelength absolute interferometry based on a cavity-enhanced electro-optic frequency comb pair," *Opt. Lett.*, vol. 39, no. 20, pp. 5834–5837, 2014.
- [9] X. Zhao, X. Qu, F. Zhang, Y. Zhao, and G. Tang, "Absolute distance measurement by multi-heterodyne interferometry using an electro-optic triple comb," *Opt. Lett.*, vol. 43, no. 4, pp. 807–810, 2018.
- [10] Y. Nakajima and K. Minoshima, "Highly stabilized optical frequency comb interferometer with a long fiber-based reference path towards arbitrary distance measurement," *Opt. Express*, vol. 23, no. 20, pp. 25979–25987, 2015.
- [11] H. Wu, F. Zhang, T. Liu, P. Balling, J. Li, and X. Qu, "Long distance measurement using optical sampling by cavity tuning," *Opt. Lett.*, vol. 41, no. 10, pp. 2366–2369, May 2016.
- [12] K.-N. Joo and S.-W. Kim, "Refractive index measurement by spectrally resolved interferometry using a femtosecond pulse laser," *Opt. Lett.*, vol. 32, no. 6, pp. 647–649, 2007.
- [13] L. J. Yang, H. Y. Zhang, Y. Li, and H. Y. Wei, "Absolute group refractive index measurement of air by dispersive interferometry using frequency comb," *Opt. Express*, vol. 23, no. 26, pp. 33597–33607, 2015.
- [14] A. Hirai and H. Matsumoto, "Low-coherence tandem interferometer for measurement of group refractive index without knowledge of the thickness of the test sample," *Opt. Lett.*, vol. 28, no. 21, pp. 2112–2114, 2003.
- [15] D. F. Murphy and D. A. Flavin, "Dispersion-insensitive measurement of thickness and group refractive index by low-coherence interferometry," *Appl. Opt.*, vol. 39, no. 25, pp. 4607–4615, 2000.
- [16] G. Bönsch and E. Potulski, "Measurement of the refractive index of air and comparison with modified Edlén's formulae," *Metrologia*, vol. 35, no. 2, p. 133, 1998.